DIGITIZATION APPROACHES FOR URBAN CULTURAL HERITAGE: LAST GENERATION MMS WITHIN VENICE OUTDOOR SCENARIOS

A. Martino [1, 3] *, E. Breggion [2, 3], C. Balletti [1], F. Guerra [2], G. Renghini [4], P. Centanni [4]

[1] Laboratorio di Cartografia e GIS, Dipartimento di Culture del Progetto, Università IUAV di Venezia, Dorsoduro 1827, 30123 Venice, Italy - (amartino, balletti)@iuav.it
[2] Laboratorio di Fotogrammetria, Dipartimento di Culture del Progetto, Università IUAV di Venezia, Dorsoduro 1827, 30123 Venice, Italy - (ebreggion, guerra2)@iuav.it
[3] Dipartimento di Ingegneria e Architettura, Università degli studi di Trieste, Via Alfonso Valerio 6/1, 34127 Trieste, Italy - (andrea.martino, enrico.breggion)@phd.units.it
[4] STONEX® Srl | Part of UniStrong, Viale dell'Industria 53, 20037 Paderno Dugnano, Italy - (Gianluca.Renghini, Paolo.Centanni)@stonex.it

KEY WORDS: Urban Cultural Heritage, 3D survey, Terrestrial Laser Scanning, Mobile Mapping System, SLAM

ABSTRACT:
This paper explores the use of Mobile Mapping Systems (MMSs) for urban Cultural Heritage (CH) documentation, which has become an increasingly important tool in surveying for rapid and accurate mapping of both internal and external environments. The study evaluates the performance of the STONEX® X120^{GO} *SLAM Laser Scanner*, a recent commercial MMS, in documenting CH in various outdoor applications, including urban environments and inaccessible places. The methodology was applied to three test fields in the historic centre of Venice, which include Piazza San Marco, Santa Marta area, and the Venetian canal called Rio de le Toresele. The STONEX® X120^{GO} *SLAM Laser Scanner* is composed of a 360° rotating head LiDAR scanner, three 5MP cameras, and an Inertial Measurement Unit (IMU) and Global Navigation Satellite System (GNSS) for geospatial 3D point cloud creation. The MMS was evaluated in terms of time, accuracy, and point cloud resolution against other active sensors such as Terrestrial Laser Scanners (TLSs) and spherical photogrammetry. The results suggest that the tested MMS has reached optimal levels of development, enabling high-speed data collection and providing good accuracy for significant urban CH sites. Overall, the paper highlights the importance and potential of MMSs for CH documentation and emphasizes the need for ongoing development to optimize the management process.

1. INTRODUCTION

Cultural Heritage (CH) is a crucial aspect of our collective human experience that serves as a reminder of our past and informs our future. Preserving and documenting CH is, therefore, of utmost importance, and this has led to the emergence of digital acquisition technologies. These technologies have made it possible to create detailed and accurate 3D models of CH sites (Barba et al., 2021; Chiabrando et al., 2022), enabling researchers and historians to study and analyze them in ways that were previously impossible. However, digital acquisition of CH is a complicated process that requires a thorough understanding of the object's peculiarities and the aim of the investigation. In recent years, the development of geomatics techniques has led to the creation of a wide variety of sensors that can be used for CH digital acquisition. These sensors range from RGB and multispectral camera both in terrestrial and aerial photogrammetry (Mathys et al., 2019), to Terrestrial Laser Scanners (TLSs), airborne LiDAR (Laser Imaging Detection and Ranging) and Mobile Mapping Systems (MMSs) based on Simultaneous Localization and Mapping (SLAM) algorithms (Rodríguez-Gonzálvez et al., 2017).
In the last years, MMSs have become increasingly important tools in surveying for the rapid and accurate mapping of both internal and external environments, thanks to their ease of use and their ability to mount them on vehicles and backpacks or simply bringing them by hand (Elhashash et al., 2022). These systems integrate and synchronize active sensors together with Inertial Measurement Unit (IMU) and Global Navigation Satellite System (GNSS) sensors in order to create geospatial 3D point cloud. One of the main benefits of portable MMSs is that they enable the gathering of a significant amount of georeferenced information rapidly and effectively, allowing for the quick and efficient digitization of even large urban areas and inaccessible places (Li et al., 2020).
The use of MMSs is particularly relevant due to the sensitivity of CH sites to external factors, such as environmental and human-induced changes. MMSs can capture rapid measurements of CH structures and objects, and the resulting point cloud data can be used for a wide range of applications, such as city mapping, architectural and urban preservation, and even virtual reconstruction. MMSs can capture data from multiple perspectives, allowing for a comprehensive view of the CH site and its surroundings. Additionally, the use of MMSs can reduce the need for manual measurements, which can be time-consuming and labor-intensive (Lagüela et al., 2018).
It should be noted that although these instruments are not new in terms of technology, they are continually being developed despite being the focus of extensive study in recent years, because there are still some challenges that need to be addressed. MMSs management process optimization has emerged as a focal topic: one such challenge is the processing of the large amounts of data generated by these systems. The data collected by MMSs is often massive, and post-processing this data requires significant computational power, a considerable amount of time and expertise. Furthermore, the accuracy and quality of the data collected by MMSs can be affected by factors such as weather conditions, signal interference, and the quality of the equipment used (Chiang et al., 2021): these elements may result in inaccurate trajectory estimation and erroneous geometry.
Another challenge in using MMSs for CH documentation is the need for careful planning and management. The use of MMSs requires a thorough understanding of the CH site and its

* Corresponding author

surroundings, as well as the objectives of the project. Proper planning and management are essential to ensure that the data collected is accurate and useful for the intended purpose.
Summarizing, the use of MMSs in urban CH digitization has great potential for preserving and documenting aims. Although while MMSs drastically cut down on the data collecting process, they still take a lot of time and resources to reconstruct optimized and filtered data (Sairam et al., 2016). However, the challenges associated with the use of MMSs need to be carefully addressed to ensure that the data collected is accurate, useful, and can be used for the intended purpose. With proper planning and management, MMSs can play a vital role in the preservation and documentation of cultural heritage.
Based on the observations presented above, the aim of this work is to evaluate the performance of one of the most recent commercial MMS for urban CH documentation within different outdoor applications (Maset et al., 2021; Nocerino et al., 2017). In detail, this paper evaluates the suitability of the MMS in various complex environments that are characterised by particular urban peculiarities by using the system by handheld walking down the streets and be taken by boat.

1.1 Urban CH case studies

The methodology was applied to three test fields (Figure 1) in the historic centre of the city of Venice: the first application concerns Piazza San Marco (a), which is not only the city's most significant place, but an example of pertinent application because it is an open urban space with constant anthropic presence; the second application regarded a Venetian canal called Rio de le Toresele (b) that could only be accessed by boat, therefore difficult to survey with more traditional methods; the third application was in the urban Santa Marta area, in Calle Larga S. Marta (c), an example of venetian narrow streets leading to wider areas, very similar to many urban contexts.

Figure 1. The three case studies: Piazza San Marco (a), Rio de le Toresele (b), Calle Larga S. Marta (c)

1.2 The STONEX® X120^{GO} *SLAM Laser Scanner*

The STONEX® X120^{GO} *SLAM Laser Scanner*[1] (Figure 2) device was the portable MMS tested in this study. It is composed by a 360° rotating head 16-channels LiDAR scanner, which can form a 270°x360° point cloud coverage acquiring 320000 pts/s in a 0.5m-120m range. Three 5MP cameras are adopted to form a horizontal 200° field of view (FOV) and a vertical 100° FOV, which can synchronously obtain texture information and to furthermore produce coloured point clouds and partial panoramic images. The STONEX® X120^{GO} *SLAM Laser Scanner* has an integrated structure design with a built-in control and storage system and built-in replaceable lithium batteries. Once pressed the start button, the device can start operations immediately, making data acquisition more efficient and convenient[2]. This system has a wealth of eternal interfaces, which can be connected to a panoramic camera, a GNSS module, a car, a Uncrewed Aerial Vehicle (UAV) and so on, to diversify data collections and adapt to more application scenarios. In the classic configuration, the instrument is equipped with a base with a sight that allows to acquire control points by placing the instrument on ground sited points. In the post-production phase, the control points can be combined with known coordinates points to georeference the scans.
The system provides a relative accuracy of 6 mm[2] according to the manufacturer's standards, however this precision can rapidly decrease depending on how effectively the SLAM algorithm performs. The characteristics of the scanned environment, the absence of loop closures on the trajectory and the procedures inaccuracy in acquisition phase can significantly affect the data reconstruction. In order to ensure the accuracy of data collection, it is important for the STONEX® X120^{GO} *SLAM Laser Scanner* devices to remain stable and avoid any sudden movements, and to prevent any obstruction from pedestrians or vehicles in front of the device during the initialization. This is applicable to all MMS devices (Tanduo et al., 2022).
The system employs two specific programs: for project management, real-time point cloud display, image preview, firmware update, and other functions, the mobile app STONEX® GO*app*[1] is specifically designed (Android operating); post-processing of gathered data, more accurate trajectory reconstruction and high-definition colour point clouds, filtering and denoising, creation of partial panoramic images, cutting, registration and optimization processing can all be done with GO*post*[1] (Windows operating system).

Figure 2. The STONEX® X120^{GO} *SLAM Laser Scanner* and the S-RTK100 Portable RTK Module

2. MATERIALS AND METHODS

The purpose of this research, as previously stated, is to analyze the performance of the STONEX® X120GO *SLAM Laser Scanner* in the field of urban CH in order to document or produce an architectural analysis. These results were investigated in three different outdoor scenarios, which are mentioned below. To be able to assess the instrument's capabilities under pressure if the rules for data collection weren't strictly followed, different approaches were used on each test field, each of which had unique and specific characteristics.

2.1 Piazza San Marco

As first case study, Piazza San Marco is presented. The square was chosen because MMS technology has the potential to provide valuable data for the documentation and digital navigation of the area, but it also presents several challenges (Di Stefano et al., 2021).

[1] https://www.stonex.it/it/project/x120go-slam-laser-scanner/

[2] STONEX® X120GO *SLAM Laser Scanner* user manual

The main problems are the great size of the square and the high density of people in the area, which can make it difficult to capture accurate and complete data. This can result in missing or distorted information, particularly in areas with heavy foot traffic. The survey campaign was entirely conducted on the morning of 2 November 2022.
Through the use of a STONEX® X100 *Laser Scanner*[3], a model of the square's three facades (the Procuratie Vecchie to the north, the Ala Napoleonica to the west, and the Procuratie Nuove to the south) was obtained in order to assess the accuracy of the handheld MMS. With an accuracy of 6 mm @ 10m, this instrument has a 360 x 268 field of view and can measure up to 3200000 points per second. The facade, which measures 298 meters in length, was surveyed using seven static scans conducted from various stations. The scans were then registered using Leica's Cyclone REGISTER 360 software using a cloud-to-cloud registration method that was optimized with the ICP (Iterative Closest Point) algorithm (Figure 3).

Figure 3. The Piazza San Marco test field acquired by the STONEX® X100 *Laser Scanner*

As regards the STONEX® X120GO *SLAM Laser Scanner*, in order to gather a surplus of overlapping scans, five different acquisition paths were made (Table 1), passing through the square (Figure 4), beneath the arcades, around the bell tower, and throughout the entire area. As previously mentioned, it is always advised to run a loop closure path when using this type of mapping system. However, the site extension made it impossible to adhere to this rule; otherwise, the acquisition time would have been too long and would have made it difficult to handle files that were excessively big. Without ever acquiring ground control points or using a Real-Time Kinematic (RTK) module, the instrument has always been carried by hand.

Dataset	Acquisition time	Trajectory distance	Mean speed
SN00056_PROJ1	13’35’’	838m	1.08m/s
SN00056_PROJ2	13’26’’	858m	1.15m/s
SN00056_PROJ3	11’42’’	704m	1.10m/s
SN00056_PROJ4	11’54’’	740m	1.13m/s
SN00056_PROJ5	12’26’’	760m	1.11m/s

Table 1. The five MMS acquisition paths' operative attributes within the Piazza San Marco test field.

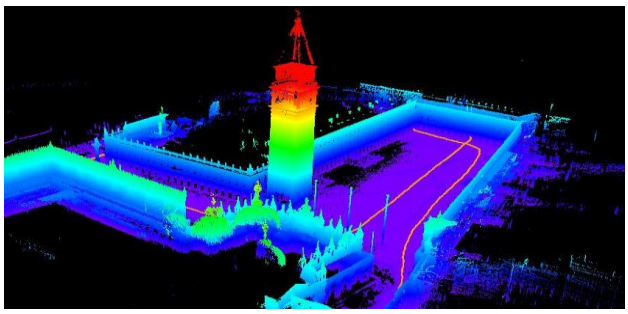

Figure 4. The Piazza San Marco first dataset acquired by the STONEX® X120GO *SLAM Laser Scanner*

The "One-click Solve" tool suggested by the manual was used during the post-processing phase in the STONEX® G*opost* software. Within this step the program enables to elaborate data by defining all the processing to be done in a single window: the selected parameters allowed the recalculation of the IMU/LiDAR trajectory more accurately, the automatic filtering of pedestrians and the optimization of the point cloud (Figure 5). Regarding the choice of the parameter "Stability", which according to the manual refers to the degree of variability of the scene, it has been set to the value of 1 for all scans.

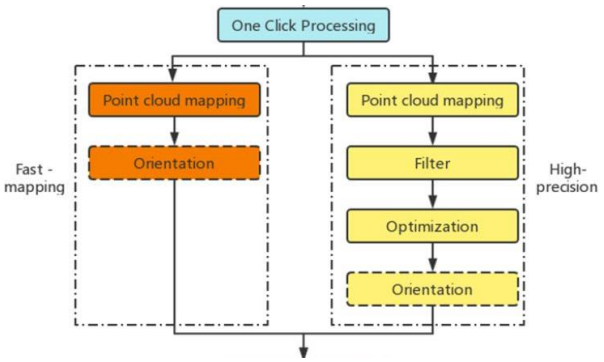

Figure 5. The MMS elaboration within the software.

All point clouds were then georeferenced using the same local reference system by homologous points detection and roto-translation. Using TLS data as a ground reference, all scans were then co-registered with the ICP algorithm after manually removing points that did not belong to the surfaces of the three facades under consideration.
Although the use and evaluation of the MMS system was the main focus of this study, datasets from spherical photogrammetry, a subject that the Venice photogrammetry laboratory has been working on for some time, were also included. A dataset of 95 images with an average step of approximately 3 meters were collected using the Ricoh Theta Z1 spherical camera at a distance of generally 8 meters from the target prospectuses. Care was taken to keep the lens system parallel to the axes while taking pictures.
Through the use of the Structure-From-Motion (SFM) software Agisoft Metashape[4] (version 2.0), the set of spherical images was processed (Figure 6). The scanning point clouds from the STONEX® X100 *Laser Scanner* were added to the structure from motion processing, blocking their alignment in a group and resetting the bundle external orientation. The pre-processed RAW images were oriented, and then the photogrammetric point cloud was rotated using the ground truth as reference.

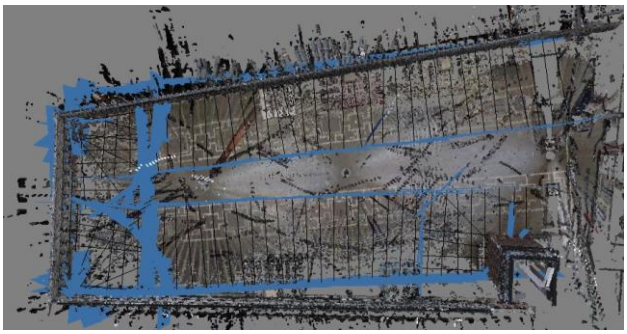

Figure 6. The spherical images orientation within the integration of the photogrammetric and TLS point clouds.

[3] https://www.stonex.it/it/project/x100-laser-scanner/#data%20sheet

[4] https://www.agisoft.com/

2.2 Rio de le Toresele

The issues related to the survey of the Rio de le Toresele's architectural facades have already been thoroughly discussed in (Breggion et al., 2022): the dataset that serves as the ground truth and the section concerning the acquisition and processing of spherical images are both allowed and then used to make comparisons with data recently obtained using the STONEX® X120GO *SLAM Laser Scanner*.
For this test field, the MMS was manually retrieved from an operator standing on a motorboat to acquire the facades. Two separate scans (Table 2) have been performed: the first, which departed from the island of San Sebastiano, passed to the south of Fondamenta Zattere, and sailed the Rio from south to north (Figure 7); the other crossing the Rio in the opposite direction, skirting the island of San Gregorio, and ending up in Canal Grande (Figure 8).

Dataset	Acquisition time	Trajectory distance	Mean speed
SN00053_PROJ1	12’41’’	1079m	1.54m/s
SN00053_PROJ2	13’24’’	1008m	1.35m/s

Table 2. The two MMS acquisition paths' operative attributes within the Rio de le Toresele test field.

The "One-click Solve" tool was used to process the acquisitions as shown in the test field above, with both projects having a “Stability” parameter of 1. SN00053_PROJ1 dataset's reconstruction failed, so the post processing of this dataset was done by trying all the values of "Stability", being able to be solved only using the value of 5.
In order to maintain consistency with the first project, the second project was post-processed initially with a Stability value of 1, then successively with a value of 5. Both these elaborations were successful.
Then, all point clouds were georeferenced using the same local reference system. After manually removing points that did not belong to the surfaces of the architectural facades of Rio de le Toresele, all scans were co-registered with the ICP algorithm using TLS data as a ground truth.

Figure 7. The Rio de le Toresele first dataset acquired by the STONEX® X120GO *SLAM Laser Scanner*; the test field is highlighted in red.

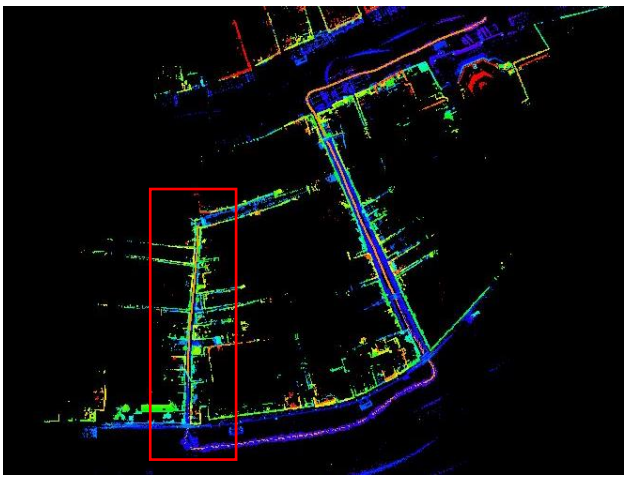

Figure 8. The Rio de le Toresele second dataset acquired by the STONEX® X120GO *SLAM Laser Scanner*; the test field is highlighted in red.

2.3 Calle Larga S. Marta

The last application was made within the urban area of Santa Marta, more specifically on an area characterized by narrow streets leading to wider areas between Calle Larga S. Marta and Calle dei Secchi. Santa Marta is a quiet and residential area, not as busy as some other neighborhoods in Venice, and there are no internal canals.
These features make this test field ideal for the use of MMSs, so the acquired STONEX® X120GO *SLAM Laser Scanner* dataset has been post-processed in various ways to test its true potential.
In order to realize the ground truth, a FARO FOCUS 3D CAM2S120[5] was used to acquire a total of 11 TLS static acquisitions with a reasonable overlap value between successive scans.
The Leica Cyclone REGISTER 360 software was used to record scans using a cloud-to-cloud recording technique that was enhanced with the ICP algorithm, just like in the Piazza San Marco case study.
The MMS acquisition resulted in a single scan (Table 3) while maintaining the strictest adherence to the methods suggested by the user manual and bibliography (Hensel et al., 2022): a multi-path and closed route was planned (Figure 9), and many closed circles were carried out, for the best possible accuracy of the data solution. In addition, the operator made sure to carry out slow movements by slowing down its walking speed in comparison to prior test fields. The last step was to acquire 4 control points placing the MMS on certain points, the coordinates of which were later determined using the STONEX® S900A Global Navigation Satellite System (GNSS) receiver using a Network Real-Time Kinematic (NRTK) approach.

Dataset	Acquisition time	Trajectory distance	Mean speed
SN000148_PROJ1	15’17’’	668m	0.77m/s

Table 3. The MMS acquisition paths' operative attributes within the third test field.

[5] https://www.faro.com/en/Products/Hardware/Focus-Laser-Scanners

Figure 9. The Calle Larga S. Marta dataset acquired by the STONEX® X120GO *SLAM Laser Scanner*; the trajectory is shown in orange dots.

The post-processing was carried out using the "One-click Solve" tool in the Go*post* software, trying to greatly vary the parameters (Table 4) in order to compare the outcomes of the elaborations and determine which outcome would have adhered more to the ground truth.

Sub-Dataset	Stability parameter	Point cloud orientate	GCP
R148-p1.1	1	Rigid	No
R148-p1.5	5	Rigid	No
R148-p1.1GCP	1	Rigid	Yes
R148-p1.5GCP	5	Rigid	Yes
N148-p1.1GCP	1	Nonrigid	Yes
N148-p1.5GCP	5	Nonrigid	Yes

Table 4. The Calle Larga S. Marta elaboration parameters.

Regarding spherical photogrammetry, the acquisition method was the same, but two photogrammetric blocks had been acquired at various heights: a dataset of 215 images with an average step of roughly 2 meters was collected using the Ricoh Theta Z1 spherical camera placed in the middle of the road.
The gathered set of images was processed using Agisoft Metashape (version 2.0). The scanning point clouds from the FARO FOCUS 3D CAM2S120 were incorporated into the structure from motion processing, blocking their alignment in a group and resetting the bundle external orientation. Finally, the photogrammetric point cloud (Figure 10) was rotated using ground truth as a reference.

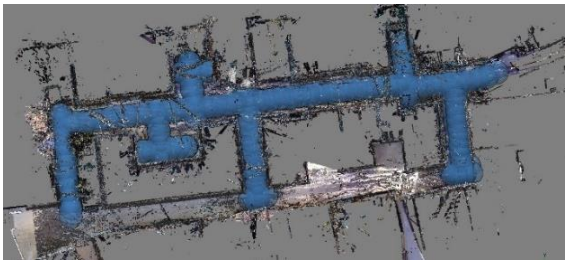

Figure 10. The spherical images orientation within the integration of the photogrammetric and TLS point clouds

3. DATASET EVALUATION AND RESULTS

Initially, the MMS and the spherical camera were evaluated in terms of number of points, density, and point cloud roughness against the most frequently used active sensors for significant cultural heritage sites documentation (Table 5, Table 6, Table 7). To assess these parameters, two different phase-shift (PS) TLSs (the FARO FOCUS 3D CAM2S120 and the Stonex X100) were employed in order to obtain reference point clouds.

Sub-Dataset	N. of points	Density	Roughness
Stonex X100	51066953	11610pts/m^2	0.004959m
56-p1.1	7451934	651pts/m^2	0.006089m
56-p2.1	4510074	1272pts/m^2	0.009742m
56-p3.1	7163691	1118pts/m^2	0.007031m
56-p4.1	2618892	2161pts/m^2	0.012894m
56-p5.1	2999579	470pts/m^2	0.006964m
RicohTheta Z1	8110313	1460pts/m^2	0.011179m

Table 5. The first test-field Sub-Dataset consistency indices.

Sub-Dataset	N. of points	Density	Roughness
FARO FOCUS	60966292	24357pts/m^2	0.002524m
53-p1.5	5654467	1915pts/m^2	0.003175m
53-p2.1	7349922	4592pts/m^2	0.003654m
53-p2.5	8544401	7343pts/m^2	0.004423m
Ricoh Theta Z1	28922961	16565pts/m^2	0.004871m

Table 6. The second test-field Sub-Dataset consistency indices.

Sub-Dataset	N. of points	Density	Roughness
FARO FOCUS	309017926	18053pts/m^2	0.001315m
R148-p1.1	25921329	4065pts/m^2	0.001998m
R148-p1.5	26008567	4102pts/m^2	0.002441m
R148-p1.1GCP	25913375	4067pts/m^2	0.001998m
R148-p1.5GCP	25991029	4100pts/m^2	0.002441m
N148-p1.1GCP	25891414	4077pts/m^2	0.002257m
N148-p1.5GCP	26161111	4130pts/m^2	0.002682m
Ricoh Theta Z1	65814596	15842pts/m^2	0.006201m

Table 7. The third test-field Sub-Dataset consistency indices.

Comparison of the generated 3D point clouds from the two technologies reveals the differences between them and highlights the errors that affect the building elements.
Firstly, the examined point clouds were finely recorded using the ICP algorithm; then, the C2C (Cloud to Cloud) distance computation methods were used to analyse the standard deviation values in the final 3D global models, and the extraction of horizontal profiles was used to investigate the geometric differences.
The results are provided below (Table 8, Table 9, Table 10).

Sub-Dataset	ICP RMSe	C2C distance	
		Mean	Std. dev.
56-p1.1	0.0262763m	0.043416m	0.051900m
56-p2.1	0.0731409m	0.094148m	0.072179m
56-p3.1	0.0526946m	0.076864m	0.070190m
56-p4.1	0.0526562m	0.078542m	0.072279m
56-p5.1	0.0327106m	0.059397m	0.072328m
RicohTheta Z1	0.0513477m	0.075034m	0.062959m

Table 8. The first test-field Sub-Dataset ICP and C2C distance computation results.

Sub-Dataset	ICP RMSe	C2C distance	
		Mean	Std. dev.
53-p1.5	0.0342994m	0.065583m	0.070956m
53-p2.1	0.0240556m	0.025557m	0.042588m
53-p2.5	0.0273772m	0.033285m	0.049008m
Ricoh Theta Z1	0.0303727m	0.023970m	0.037793m

Table 9. The second test-field Sub-Dataset ICP and C2C distance computation results.

Sub-Dataset	ICP RMSe	C2C distance	
		Mean	Std. dev.
R148-p1.1	0.0353977m	0.018598m	0.034760m
R148-p1.5	0.0351090m	0.017818m	0.034877m
R148-p1.1GCP	0.0353282m	0.018554m	0.035030m
R148-p1.5GCP	0.0351378m	0.017889m	0.034922m
N148-p1.1GCP	0.0392290m	0.025178m	0.035376m
N148-p1.5GCP	0.0395168m	0.025471m	0.035084m
Ricoh Theta Z1	0.0469795m	0.037499m	0.047829m

Table 10. The third test-field Sub-Dataset ICP and C2C distance computation results.

In order to remove pedestrian data that might get worse the outcome, the distance in the dataset for Piazza San Marco was recalculated using only the surfaces of the three facades. By taking this precaution, the sub-datasets with the best results are enhanced (Table 11).

Sub-Dataset	C2C distance	
	Mean	Std. dev.
56-p1.1	0.032836m	0.023873m
56-p2.1	0.099082m	0.073311m
56-p3.1	0.069425m	0.065838m
56-p4.1	0.078867m	0.072192m
56-p5.1	0.040898m	0.046393m
RicohTheta Z1	0.064141m	0.058019m

Table 11. The first test-field Sub-Dataset ICP and C2C distance computation results after the floor removal.

Finally, the same analysis was carried out experimentally using data from the MMS as ground truth, comparing the point clouds obtained with spherical photogrammetry, following the procedures described above. Only the best elaborations were used in the operation, which was carried out once for each dataset (Table 12).

Sub-Dataset	ICP RMSe	C2C distance	
		Mean	Std. dev.
56-p1.1 Ricoh Theta Z1	0.0413782m	0.065445m	0.047833m
53-p2.1 Ricoh Theta Z1	0.0231298m	0.025862m	0.023827m
R148-p1.5 Ricoh Theta Z1	0.0382544m	0.039221m	0.041427m

Table 12. MMS-Spherical Photogrammetry ICP and C2C distance computation results.

4. DISCUSSIONS AND CONCLUSIONS

The ICP RMS errors and the C2C absolute distances between the point clouds were calculated as a first quantitative comparison between the portable MMS model and the TLS one using CloudCompare[6]. Only distances of less than 50 cm were considered in order to prevent points belonging to surfaces not scanned by one of the sensors from having unrealistic values.
First of all we focused on the results on the results obtained in the Piazza San Marco case study. Outcomes were considered unexpectedly positive given that the acquisitions' goal was not analytical but rather documentary and demonstrative. As a consequence, the acquisitions were completed as quickly as possible while attempting to gather as much information as possible about a much wider area than that on which the quantitative analysis was conducted. Out of the 5 acquisitions, the first and fifth in particular produced positive results in terms of analysis. Due to its greater completeness in terms of point quantity and density, sub-dataset 56-p1.1 was determined to be the best. 56-p1.1 and 56-p5.1 are comparable from a noise perspective (Figure 11, Figure 12). When the acquisition trajectories for these two datasets are analyzed, they are the only ones that traverse the centre of the square; in particular, the 56-p1.1 crosses it twice in reverse, nearer the facades of the buildings. The comparison test between the MMS data and the photogrammetric cloud produced some quite positive results in this instance, particularly for the dataset expansion. It should be noted that the cloud from spherical photogrammetry is complete and of good quality only in correspondence of the acquisition high and in the more closely acquired zones (Figure 13).

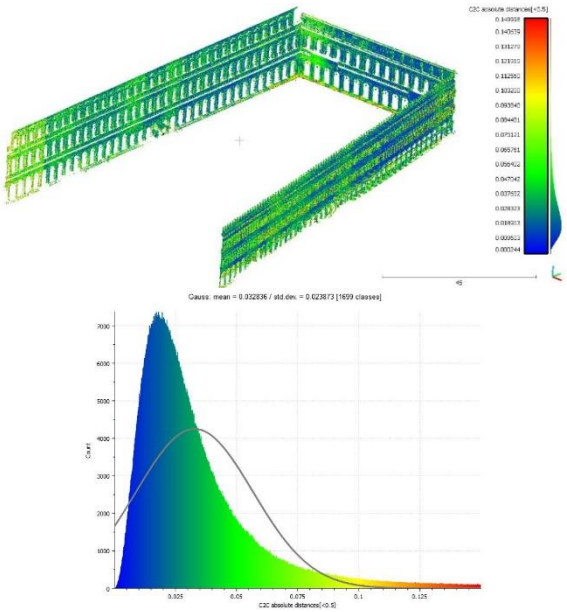

Figure 11. Sub-Dataset 56-p1.1 C2C distance computation.

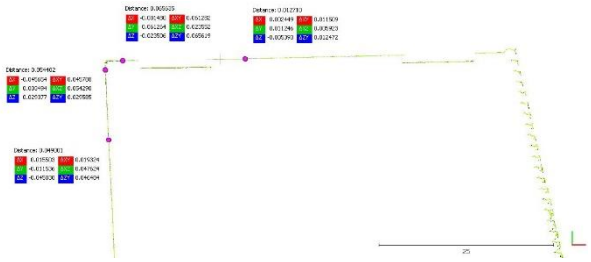

Figure 12. Sub-Dataset 56-p1.1 horizontal profiles.

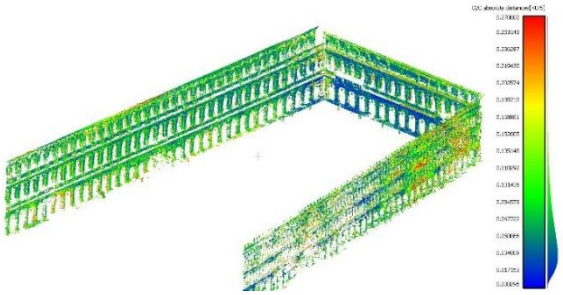

Figure 13. Sub-Dataset 56-p1.1-Ricoh Theta Z1 photogrammetric point cloud C2C distance computation.

The second test filed produced better results since the investigated area was much smaller than the first test filed and because the distance between the facades of the opposing

[6] https://www.danielgm.net/cc/

buildings was, on average, only 4 to 6 meters. The main challenges were with the acquisition techniques because the motion of the boat is unusual for these instruments and can cause misalignments. Another factor that must be considered is the boat's speed and how hard it is to maintain a stable trajectory. The first sub-dataset, which is connected to the first acquisition, yields the worst outcomes. The boat was traveling at a faster speed and collected fewer points in this acquisition, as can be seen. For the second acquisition, performed at a lower speed, the best result was obtained with a Stability parameter equal to 1 (Figure 14, Figure 15). It is possible that the above-mentioned elements, specifically speed and stability, have impacted these outcomes. Additionally, the test field was acquired immediately after the instrument initialization phase in the second acquisition, whereas it was acquired during the trajectory's end in the first acquisition. Excellent results were obtained from the comparison test between the MMS data and the photogrammetric cloud (Figure 16), but the issue of the data's completeness in relation to the camera's height at the time of acquisition still exists.

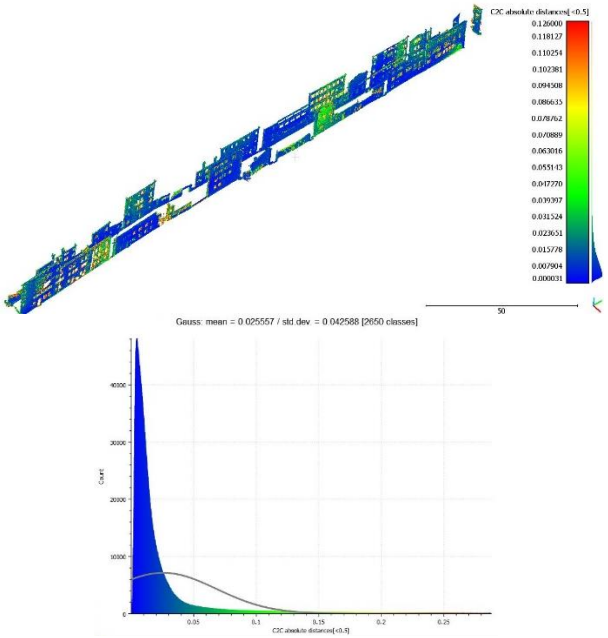

Figure 14. Sub-Dataset 53-p2.1 C2C distance computation.

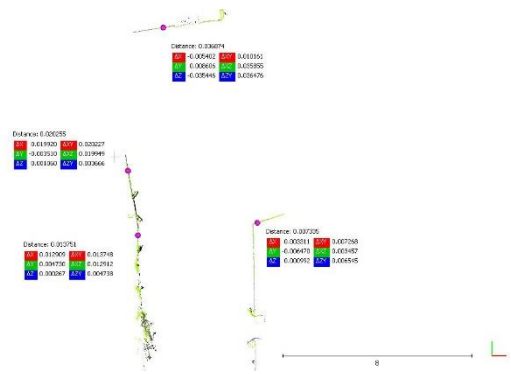

Figure 15. Sub-Dataset 53-p2.1 horizontal profiles.

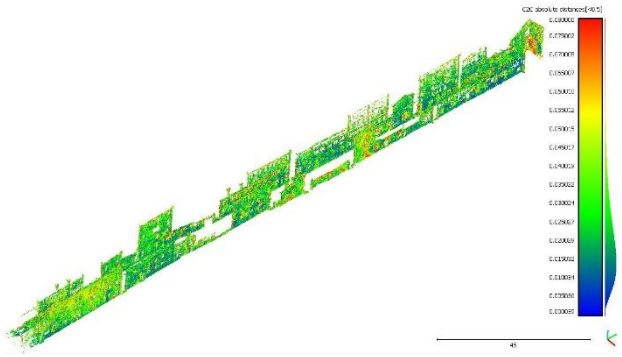

Figure 16. Sub-Dataset 53-p2.1-Ricoh Theta Z1 photogrammetric point cloud C2C distance computation.

The third test field also produced very good results. The acquisition phase was carried out much more carefully, despite the size of the acquired area being quite large. The acquisition speed was slowed down, loops were made, the path was closed at the same initialization point, and the LiDAR front was always pointed in the direction of the buildings. Using the GCP within the elaboration phase, the outcomes resulting from the "Non-Rigid" mode elaboration have been not as good as the “Rigid” ones. However, the same dataset performed better in "Rigid" mode, without using GCP, with a Stability parameter of 5 (Figure 17, Figure 18). Two conclusions can be drawn from these results: first, GCPs must be used cautiously, taking into account both the GNSS acquisition aproach accuracy and the scanning location, and second, the "stability" parameter is actually influenced by the scene's degree of variability as reported in the user manual. The comparison test between the MMS data and the spherical photogrammetric cloud produced positive results (Figure 19), but the issue of data completeness in relation to the camera height at the time of acquisition is still an issue. The values are worse in comparison to the second test field, which is consistent with the greater distance between architectural fronts.

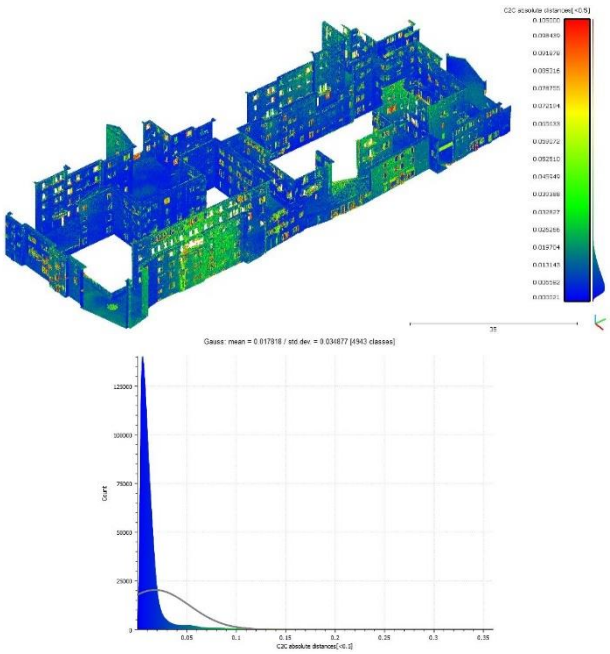

Figure 17. Sub-Dataset R148-p1.5 C2C distance computation.

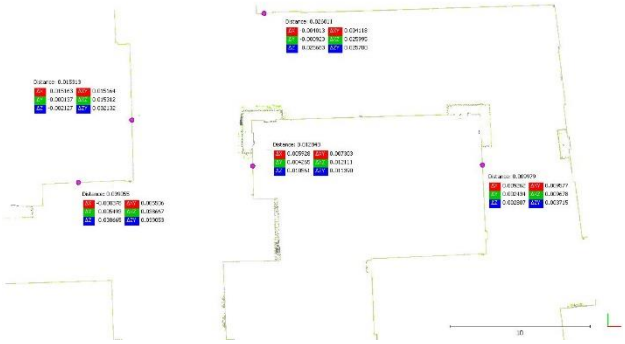

Figure 18. Sub-Dataset R148-p1.5 horizontal profiles.

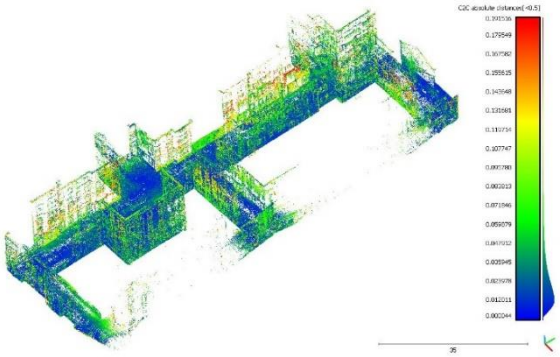

Figure 19. Sub-Dataset R148-p1.5-Ricoh Theta Z1 photogrammetric point cloud C2C distance computation.

The above-mentioned results suggest that the tested MMS has reached optimal levels of development, enabling high-speed data collecting and providing good accuracy for significant urban CH sites. As with all MMSs, careful consideration must be given to survey planning in accordance with the survey's site and objectives. In order to get the best results from these devices, consolidated best practices should always be used.

The outcomes of the tests performed using the spherical cameras are encouraging. Depending on the success of a survey and the scale of representation required, by using the former as the ground truth, data from MMS and spherical photogrammetry can be compared, and integration can make up for acquisition-phase issues.

Within test-fields with very different characteristics and using the instrument in various ways, the results obtained in the specific case of the STONEX® X120^{GO} *SLAM Laser Scanner* showed to be excellent.

REFERENCES

Barba, S.; Ferreyra, C.; Cotella, V.A.; di Filippo, A.; Amalfitano, S., 2021. A SLAM Integrated Approach for Digital Heritage Documentation, in: Rauterberg, M. (Ed.), Culture and Computing. Interactive Cultural Heritage and Arts, Lecture Notes in Computer Science. Springer International Publishing, Cham, pp. 27–39. https://doi.org/10.1007/978-3-030-77411-0_3

Chiabrando, F.; Patrucco, G.; Rinaudo, F.; Sammartano, G.; Scolamiero, V.; Vileikis, O.; Hasaltun Wosinski, M. 3D DOCUMENTATION TOWARDS HERITAGE CONSERVATION: A RAPID MAPPING APPROACH APPLIED TO BAHRAIN FORTS, Int. Arch. Photogramm. Remote Sens. Spatial Inf. Sci., XLIII-B2-2022, 769–776

Mathys, A.; Jadinon, R.; Hallot, P., 2019. EXPLOITING 3D MULTISPECTRAL TEXTURE FOR A BETTER FEATUREIDENTIFICATION FOR CULTURAL HERITAGE. ISPRS Ann. Photogramm. Remote Sens. Spatial Inf. Sci. IV-2/W6, 91–97. https://doi.org/10.5194/isprs-annals-IV-2-W6-91-2019

Rodríguez-Gonzálvez, P.; Jiménez Fernández-Palacios, B.; Muñoz-Nieto, Á.; Arias-Sanchez, P.; Gonzalez-Aguilera, D., 2017. Mobile LiDAR System: New Possibilities for the Documentation and Dissemination of Large Cultural Heritage Sites. Remote Sensing 9, 189. https://doi.org/10.3390/rs9030189

Elhashash, M.; Albanwan, H.; Qin, R., 2022. A Review of Mobile Mapping Systems: From Sensors to Applications. Sensors 22, 4262. https://doi.org/10.3390/s22114262

Li, S.; Li, G.; Wang, L.; Qin, Y. SLAM integrated mobile mapping system in complex urban environments. ISPRS J. Photogramm. Remote. Sens. 2020, 166, 316–332

Lagüela, S.; Dorado, I.; Gesto, M.; Arias, P.; González-Aguilera, D.; Lorenzo, H. Behavior Analysis of Novel Wearable Indoor Mapping System Based on 3D-SLAM. Sensors 2018, 18, 766. https://doi.org/10.3390/s18030766

Chiang, K.W.; Tsai, GJ.; Zeng, J.C. (2021). Mobile Mapping Technologies. In: Shi, W., Goodchild, M.F., Batty, M., Kwan, MP., Zhang, A. (eds) Urban Informatics. The Urban Book Series. Springer, Singapore. https://doi.org/10.1007/978-981-15-8983-6_25

Sairam, N.; Nagarajan, S.; Ornitz, S., 2016. Development of Mobile Mapping System for 3D Road Asset Inventory. Sensors 16, 367. https://doi.org/10.3390/s16030367

Maset, E.; Cucchiaro, S.; Cazorzi, F.; Crosilla, F.; Fusiello, A.; Beinat, A., 2021. INVESTIGATING THE PERFORMANCE OF A HANDHELD MOBILE MAPPING SYSTEM IN DIFFERENT OUTDOOR SCENARIOS. Int. Arch. Photogramm. Remote Sens. Spatial Inf. Sci. XLIII-B1-2021, 103–109. https://doi.org/10.5194/isprs-archives-XLIII-B1-2021-103-2021

Nocerino, E.; Menna, F.; Remondino, F.; Toschi, I.; Rodr´ıguezGonzalvez, P., 2017. Investigation of indoor and outdoor per-´formance of two portable mobile mapping systems. Videometrics, Range Imaging, and Applications XIV, 10332, International Society for Optics and Photonics, 103320I

Tanduo, B.; Martino, A.; Balletti, C.; Guerra, F. New Tools for Urban Analysis: A SLAM-Based Research in Venice. Remote Sens. 2022, 14, 4325. https://doi.org/10.3390/rs14174325

Di Stefano, F.; Torresani, A.; Farella, E.M.; Pierdicca, R.; Menna, F.; Remondino, F. 3D Surveying of Underground Built Heritage: Opportunities and Challenges of Mobile Technologies. Sustainability 2021, 13, 13289. https://doi.org/10.3390/su132313289

Breggion, E.; Tanduo, B.; Martino, A.; Vernier, P.; Guerra, F., 2022. La fotogrammetria sferica in ambienti complessi: il caso del Rio veneziano de le Toresele.

Hensel, S.; B. Marinov, M.; Obert, M. 3D LiDAR Based SLAM System Evaluation with Low-Cost Real-Time Kinematics GPS Solution. Computation 2022, 10, 154. https://doi.org/10.3390/computation10090154